

Zero valent iron-mediated rapid removal of bis-azo dye in solution amended with dyebath additives: Biphasic kinetics and modelling

Raja Kumar and Alok Sinha[†]

Department of Environmental Science & Engineering, Indian School of Mines, Dhanbad-826004, Jharkhand, India
(Received 20 February 2016 • accepted 30 June 2016)

Abstract–The effect of widely used dye-bath additives, namely sodium chloride, ammonium sulfate, urea, acetic acid and citric acid, on the reductive removal of azo dye AR73 by zero valent iron was investigated. Na⁺ induced ‘salting out’ effect on the dye molecules complemented with Cl[−] induced pitting corrosion of ZVI surface led to improved dye removal rate with increasing NaCl concentration. ‘Salting out’ effect of (NH₄)₂SO₄ together with enhanced iron corrosion by aggressive SO₄^{2−} and reducing effect of ‘sulfate green rust’ benefitted the reaction rates. However, beyond 1,000 mg/L (NH₄)₂SO₄ concentration, complex formation of NH₄⁺ and SO₄^{2−} with iron oxides compromised ZVI reactivity. Urea inhibited the reaction by its chaotropic effect on the dye solution and also by wrapping the ZVI surface. Enhanced iron corrosion by organic acids improved the reaction rates. The dye removal followed biphasic kinetics with initial rapid phase, when more than 95% dye removal was observed in all the studies, followed by a slow phase. The experimental data could be well evaluated using biphasic rate equation (R²>0.995 in all the cases). Highest dye removal rate of 0.900 min^{−1} was achieved at pH 2 with all the additives amended. AR73 removal could be modelled using biphasic model considering the individual effect of each additive. Rapid dye reduction capability at varied solution composition makes ZVI more advantageous and promising for wastewater treatment.

Keywords: Acid Red 73(AR73), Biphasic Kinetics, Dye-bath Additives, Modelling, Zero Valent Iron (ZVI)

INTRODUCTION

Azo dyes are a major class of synthetic, colored organic compounds that are widely used in textile dyeing. During dyeing operations, about 15% of these dyes remain unfixed to the fabric and end up in wastewaters [1]. The release of colored effluent in the ecosystem is a dramatic source of aesthetic pollution, eutrophication, and perturbations in aquatic life. These dyes are intentionally synthesized to have an electron deficient chemical structure that accounts for their low reactivity, thus making them resistant towards conventional treatment processes. Moreover, large quantities of chemical additives are complemented to the dye-bath during dyeing operations to achieve optimum color fixation onto the textile fibre. These salts pass into the wastewater with the unfixed dye and may influence the effluent treatment process.

The major techniques for treating dye wastewater include adsorption [2-7], photo-chemical degradation [8], AOPs [9], biological degradation [10]. Although extensive, there is scant knowledge on the effect of the dye-bath additives on the efficiency and kinetics of these technologies. Today, there is no convincing explanation of how these additives affect the physico-chemical techniques employed for textile dyeing effluent treatment. Zero-valent iron (ZVI or Fe⁰) is one such environmental friendly, cost effective, reusable and easy to operate treatment approach capable of destroying recalcitrant organic pollutants in water and has been widely studied to treat

wastewater containing chlorinated aliphatics [11], chlorinated aromatics [12,13], heavy metals [14] and organic dyes [15-19]. Treatment of azo dyes by ZVI was suggested because in the presence of ZVI the electron-withdrawing moieties get reductively transformed and the resulting by-products are more amenable to biological treatment processes (Eq. (1)) [18].



Contaminant reduction by ZVI is a surface mediated process and is most likely to get affected by the chemistry of dye-bath effluent. The presence of dye-bath additives might affect the reactivity of ZVI by affecting its corrosion behavior, forming precipitate on the metal surface, and/or by competing with dye molecules for the reactive sites on the metal surface.

Therefore, the present study was conducted to find the effects of commonly used dye-bath additives, including sodium chloride, ammonium sulfate, urea, acetic acid and citric acid, on the removal kinetics of bis-azo dye C.I. Acid Red 73 by ZVI. An azo dye was selected for this study because azo class of dyes are most commonly used in dyeing operations [18,20]. Synthetic dye solution was prepared and the concentration of additives was varied according to their occurrence in the textile effluent as reported in the literature. The efficiency of ZVI to remove azo dye from solution in the presence of all these additives at their highest studied concentration was also examined and the dye removal process was modelled. This is the first ever comprehensive study on the effect of dye-bath constituents on the kinetics of azo dye reduction using ZVI, and for the first time an attempt has been made to model the discoloration process. This study is expected to further enhance the existing

[†]To whom correspondence should be addressed.

E-mail: aloksinha11@yahoo.com

Copyright by The Korean Institute of Chemical Engineers.

knowledge on the effectiveness of ZVI for removal of surface water contaminants that can be beneficial in developing the practical utility of ZVI.

EXPERIMENTAL

1. Materials and Reagents

Commercially available bis-azo dye C.I. Acid Red 73 (1,3-Naphthalenedisulfonic acid, 7-hydroxy-8-[[4-(phenylazo) phenyl]azo]-, disodium salt; M.F: $C_{22}H_{14}N_4Na_2O_7S_2$; M.W: 556.48) was purchased from Atul Ltd. (India) and used without any purification. Analytical reagent grade concentrated hydrochloric acid, sodium chloride, ammonium sulfate, urea, citric acid, acetic acid and sodium hydroxide were purchased from Merck (India) and deionized (Milli Q) water was used to make all the solutions.

ZVI was prepared by method described by Kumar and Sinha [18]. Commercially available iron rod was chipped on a lathe machine and then ground into iron filings in a dough-size ball mill. The filings were sieved, and those between 40 (425 μm) and 80 (212 μm) mesh sizes were retained for use. Iron filings, thus produced, were washed 5-6 times with N_2 -sparged 1N HCl with periodic shaking, then rinsed 10-12 times with N_2 -sparged deionised (Milli Q) water. Again they were rinsed twice with 95% pure ethanol and dried for 1 hour. This treatment yielded black ZVI filings with no visible rust on the surface. ZVI was stored in a vacuum desiccator until use in various experiments. BET (Brunauer Emmett Teller) specific surface area of the dry ZVI filings was determined by BET (Brunauer Emmett Teller) surface area analyzer (NOVA 4000e, Quantachrome Instruments, USA) to be 2.16 m^2/g .

2. Experimental Method and Analysis

Batch experiments were conducted in replicate 35 mL capacity borosilicate glass vials with screw caps (Borosil, India). The concentration of Acid Red 73 (AR73) dye and ZVI was kept constant at 100 mg/L and 57.12 g/L, respectively, for all the experiments and only the concentration of additives and acids used was varied as per experimental need. For experiments using NaCl, $(\text{NH}_4)_2\text{SO}_4$ and urea, 0.5 M HCl was used to adjust the initial solution pH to 3. In studies investigating the effect of organic acids, concentrated acetic acid and/or 5 M citric acid were used to adjust solution pH, while for other experiments it is described in the respective section. Separate AR73 dye calibration curves were prepared using HCl (at pH 3), organic acids (at pH 2, 3, 4 and 5) and 1 M NaOH (at pH 9) to avoid any unexpected error while quantification of color. For proper mixing, the vials were shaken on an end-to-end tumbler (Rotospin, Tarsons, India) at 30 rpm. Shaking was conducted in dark room to prevent any kind of photo-catalytic activity. The ambient temperature was $25 \pm 2^\circ\text{C}$ for all experiments. At definite elapsed times, two replicate vials were sacrificed along with a blank and supernatants from each vial were filtered through GF/C filter paper (1.2 μm nominal pore size, Whatman, Springfield Mill, England). The filtrate was used for quantification of color using a UV spectrophotometer (UV-1800 series, Shimadzu, Japan) at the predetermined λ_{max} of 509.5 nm specific for AR73. Atomic Absorption Spectrometer (GBS Avanta, GBC Scientific Equipment, USA) was used for determination of dissolved iron content.

A scanning electron micrograph of the ZVI surface was obtained

utilizing the scanning electron microscope (FE-SEM-Zeiss, Supra 65, Germany). FTIR analysis of samples was performed using a Fourier transform infrared spectroscope (Perkin Elmer, Spectrum One, USA). The used ZVI were dried under N_2 atmosphere immediately after sampling to prevent oxidation. The N_2 dried filings were finely ground to powder form with pure KBr (5:95 ratio) (BDH chemicals, UK) and pressed into translucent pellets using a laboratory press applying 40 MPa pressure for 50 sec. Of the KBr pellets, thus obtained, FTIR scans were carried out at the mid IR region spanning from 400 cm^{-1} to $4,000\text{ cm}^{-1}$ at 16 scan speed.

3. Dye Removal Kinetics

Preliminary experimental results showed very rapid dye removal in the first 5 min followed by a slow down for the rest of the experimental duration. Evidently, the dye removal was biphasic and hence, the kinetics was elucidated using biphasic kinetic equation (Eq. (2)) given below:

$$C = C_1 e^{-k_1 t_1} + C_2 e^{-k_2 t_2} \quad (2)$$

where C is the concentration at time t, C_1 and C_2 are the dye concentration at $t=0$ min and $t=5$ min, respectively; t_1 is the initial rapid reaction phase (i.e. first 5 min) and t_2 is the slow reaction phase (from 5 min to 120 min). k_1 and k_2 are the pseudo-first order dye removal rates observed for the first 5 min and after 5 min, respectively, the values of which was determined by non-linear regression of the obtained experimental data.

RESULTS AND DISCUSSION

1. Effect of Sodium Chloride

The effect of NaCl on AR73 reductive removal is shown in Fig. 1. The dye removal data fitted well with the biphasic kinetic equation exhibiting high values of regression coefficient (see Table 1). Very rapid dye removal was achieved within first 5 min, when more than 95% dye was removed, followed by a slow removal phase (Fig. 1 inset). The dye removal accelerated noticeably with the increase in NaCl concentration from 0 g/L to 6 g/L. Using 6 g/L NaCl con-

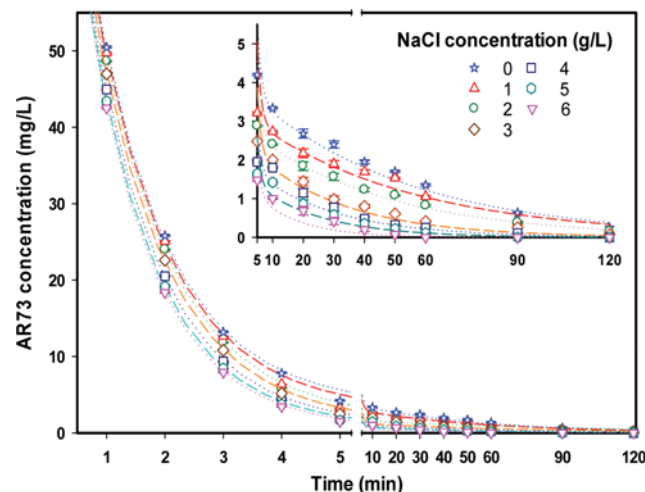


Fig. 1. Removal of AR73 by ZVI at different NaCl concentrations. Inset figure shows the temporal variation in dye concentration after 5 min.

Table 1. Biphasic AR73 removal rates in the presence of different salt concentration

Dye-bath additives	Concentration (mg/L)/pH	Removal rate (min^{-1})		R^2
		Initial 5 min	After 5 min	
Sodium chloride	0	0.736	0.017	0.997
	1	0.772	0.019	0.998
	2	0.788	0.022	0.999
	3	0.812	0.033	0.999
	4	0.848	0.037	0.999
	5	0.876	0.045	1.000
	6	0.892	0.069	1.000
Ammonium sulfate	0	0.736	0.017	0.997
	100	0.746	0.045	0.998
	300	0.763	0.047	0.998
	500	0.792	0.051	0.999
	1000	0.861	0.053	0.999
Urea	0	0.736	0.017	0.998
	10	0.722	0.017	0.997
	30	0.713	0.016	0.993
	50	0.703	0.016	0.988
	75	0.677	0.015	0.983
	100	0.660	0.012	0.972

centration, dye removal of more than 98.50% and k_1 as high as 0.892 min^{-1} was observed within first 5 min. The byproducts of AR73 dye reduction were identified and quantified by HPLC and LC-MS/MS (data not shown). These by-products are aromatic amines which originate due to reductive splitting of two azo linkages of AR73 in the presence of ZVI.

The rate enhancing effect of NaCl mainly resulted from the effect of Na^+ on the dye molecules in the bulk solution while Cl^- could affect both the bulk solution as well as the ZVI surface. The standard reduction potential of Na^+ (2.71 V) is less than that of Fe^{2+} (0.44 V); hence, it could hardly affect the degradation reactivity of ZVI [21] and Cl^- is expected to impart a major effect on the reactivity of the ZVI surface.

NaCl exhibits 'salting out' effect on the bulk dye solution that affects the solubility of azo dye. The Na^+ ions reduce the repulsion between the negative charges of dye molecules, bringing them closer to form dye aggregates [20]. Reduced solubility of the dye enhances its partitioning onto the ZVI surface [22].

Chloride anion improves the conductivity of the dye solution. The resulting increased kinetic energy and molecular motion accelerates mass transport rate of dye molecules onto the iron surface. Moreover, Cl^- is a corrosion promoter that induces pitting and crevice corrosion on the metal surface [23]. This prevents the passivation of iron surface and the metal continues to dissolve at a high rate as per Eqn. (3), (4) and (5) below:

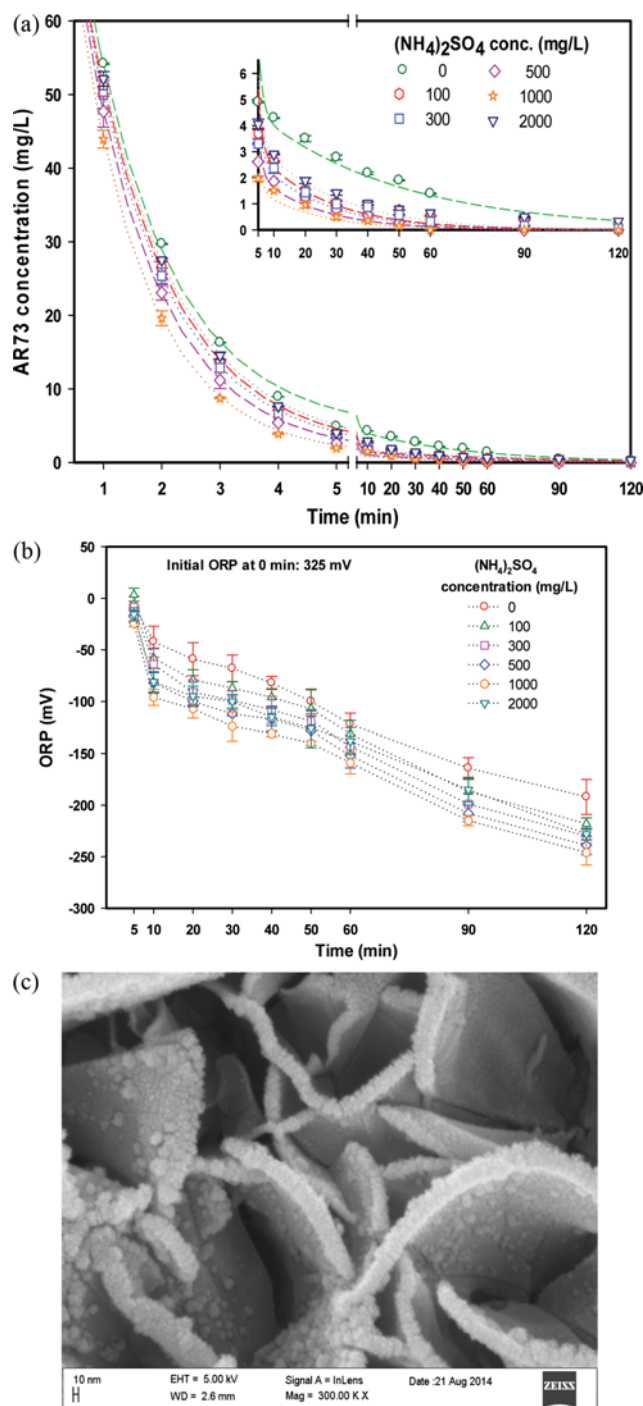
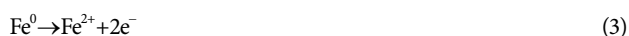


Fig. 2. (a) Removal of AR73 by ZVI at different ammonium sulfate concentrations. Inset figure shows the temporal variation in dye concentration after 5 min; (b) temporal variation of solution ORP after 5 min of AR73 treatment; (c) FE-SEM image of greenish suspended particles observed in the experiment.



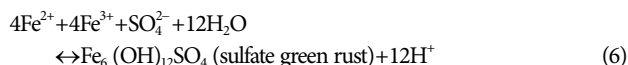
$\text{Fe}(\text{OH})_2$ formed in Eq. (5) is not passivating in nature and the produced HCl further inhibits formation of a passivating oxide/hydroxide film by dissolution of iron metal to form ferrous or fer-

ric chloride [24]. This pitting mechanism is more severe in acidic conditions when it forms deeper and larger pits [25] that provide increased surface area for dye reduction. Furthermore, pitting corrosion becomes much more intense with an increase in NaCl concentration [25]; hence, dye removal is also accelerated in a similar fashion. Also, it has been demonstrated that the solubility of oxygen (O_2) in the solution decreases with increasing chloride concentration [26]. Therefore, chloride ions can also affect the corrosion process by changing ionic strength of the electrolyte, especially when O_2 is directly involved in iron passivating reactions. Thus, Cl^- greatly accelerates dye removal rates by continuously making rejuvenated iron surface available for the reaction, increasing the iron surface area and generating more electrons for the reaction.

2. Effect of Ammonium Sulfate

Sulfate compounds are commonly used as a promoter and buffering agent in the dyeing industry. The effect of sulfate in the discoloration of azo dyes was studied using different concentrations of sulfate from 100 mg/L to 2,000 mg/L in the form of ammonium sulfate $[(NH_4)_2SO_4]$. The results, as shown in Fig. 2(a) and Table 1, indicate that amending dye solution with ammonium sulfate improved the dye discoloration removal up to a certain concentration beyond which the dye removal efficiency and rate is retarded. The dye removal followed similar biphasic pattern and highest removal efficiency (98%) and k_1 of 0.861 min^{-1} was achieved within 5 min using $(NH_4)_2SO_4$ concentration of 1,000 mg/L. The efficiency declined with further increase in $(NH_4)_2SO_4$ concentration to 2,000 mg/L. Similar effect of SO_4^{2-} has also been reported by Fan and co-workers [27].

The reason for rate enhancing effect of $(NH_4)_2SO_4$ could be its 'salting out' effect similar to NaCl onto the dye molecules in the bulk solution. Also, the aggressive nature of sulfate anion has previously been shown to enhance the reactivity of ZVI [23]. Furthermore, formation of sulfate 'green rust' could have acted as an additional reducing agent. Green rust appeared shortly after contact of ZVI with sulfate amended solution (Eq. (6)) and remained for the entire duration of the experiments. The measured potential conditions were more reducing (Fig. 2(b)). FE-SEM analyses of surface morphology of green rust reveal them to be of sjogrenite-pyroaurite class (Fig. 2(c)) [28]. It has been reported that the green rust does not prevent electron transfer [29] and may further act as a reductant. Therefore, it may account for enhanced discoloration occurring in the presence of sulfate. Choi et al. [30] and Remy et al. [31] also reported the reduction of nitrate and methyl red, respectively, in the presence of green rust.



With regard to NH_4^+ , it may form $[(Fe(NH_3)_6]^{2+})$ complex with iron that may control the concentration gradients of Fe^{2+} and Fe^{3+} at the iron-water interface and increase the solubility of ZVI. However, higher concentrations of NH_4^+ have proved to be detrimental for the surface reaction [27] and could account for lower rates at 2,000 mg/L $(NH_4)_2SO_4$ concentration. Another plausible explanation for decreased rates could be that ZVI have a positively charged oxide surface which is under the isoelectric point, and anions hav-

ing atoms with a lone pair of electrons can be adsorbed onto the surface of the particles via coordinate bond forming both outer-sphere and inner-sphere surface complexes [32]. Therefore, SO_4^{2-} anions could compete with dye molecules for the reactive sites on the iron surfaces since they have similar anionic structure, thus leading to fall in AR73 conversion rate.

The enhancement in AR73 removal was less pronounced in the presence of sulfate compared to chloride, possibly because the reported sequence for ZVI-mediated contaminant reduction rate for the Cl^- and SO_4^{2-} ligands is also opposite the sequence for the strength or affinity of the surface complexation of these inorganic ligands with iron oxides, i.e., chloride < sulfate [33]. This implies that Cl^- does not adsorb easily to iron oxides while SO_4^{2-} readily form complexes that could compromise the mass transfer process.

3. Effect of Urea

Urea is used in the dye bath to increase the solubility of the dye that enables more uniform dyeing and increased color yield. It acts as a hydrotropic agent that forms amphiphilic bridge between the solubilized dye and the aqueous media [34], thereby increasing the aqueous solubility of dyes. Fig. 3(a) and Table 1 indicate that the rate of AR73 removal retarded monotonically with increasing urea

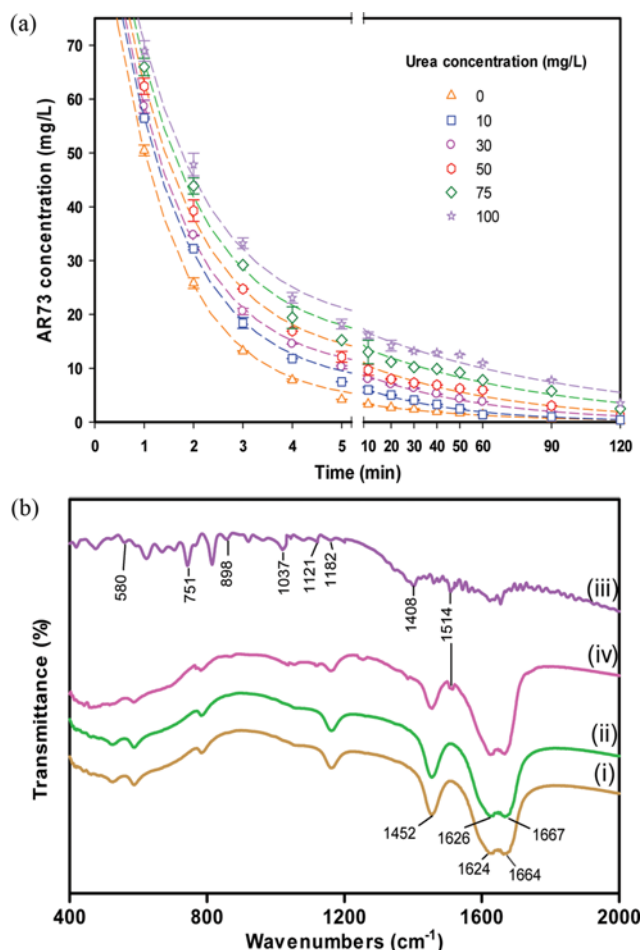


Fig. 3. (a) The degradation of AR73 by ZVI at different urea concentrations (b) FTIR spectra of (i) urea, (ii) ZVI/urea, (iii) ZVI/urea/AR73, (iv) ZVI/urea/AR73.

concentration from 10 mg/L to 100 mg/L in the dye solution. While in the control experiment 95.80% AR73 was removed within 5 min, the dye removal was recorded only 82% in the solution amended with 100 mg/L of urea.

Such negative effect can be attributed to physico-chemical effect of urea in the bulk solution as well as on the ZVI surface. In the bulk phase, chaotropic effect of urea weakens the hydrophobic effect of dye molecules, thereby inhibiting their aggregate forming ability (converse effect to NaCl). This increases the number of monomer species [22] of dye molecules, and thus the aqueous solubility of the dye molecules is enhanced and their partitioning onto the iron surface is impaired. 'Salting in' effect of urea has also been reported to modify the interaction between water and organic molecules, leading to increased free energy of adsorption [35], thereby enhancing aqueous stability of dye molecules and retarding their partitioning onto the iron surface.

Furthermore, urea could deteriorate the reactivity of ZVI by forming a wrapping film around iron surface. Urea has a property of self-association that results in directional network morphology in aqueous solution [36,37]. This network may form an even coating on the iron surface, thus creating a steric hindrance effect that prevents the access of dye molecules to the reactive sites and hinders the mass transfer process. This hypothesis warranted further investigation on the interaction of urea, AR73 and ZVI using FTIR, the results of which are presented in Fig. 3(b). Spectra of pure urea, shown in Fig. 3(b)-(i), exhibited vibration bands $\nu_{\text{C=O}}$ at wavenumber $1,667\text{ cm}^{-1}$, δ_{NH_2} bending vibration at $1,626\text{ cm}^{-1}$ and $\nu_{\text{C=N}}$ at $1,455\text{ cm}^{-1}$ which right shifts to $1,664\text{ cm}^{-1}$, $1,624\text{ cm}^{-1}$ and $1,452\text{ cm}^{-1}$ after its adsorption to ZVI (refer Fig. 3(b)-(ii)). This suggests interaction between iron surface and urea (O-Fe and N-Fe). The spectra of AR73 dye adsorbed onto the iron surface depicted in Fig. 3(b)-(iii) show intense band at $1,514\text{ cm}^{-1}$ attributable to the $-\text{N}=\text{N}-$ bond vibrations. The peaks at $1,037$ and $1,121\text{ cm}^{-1}$ are ascribed to coupling between benzene mode and $\nu_s(\text{SO}_3)$ [38], and those at $1,182\text{ cm}^{-1}$ and $1,408\text{ cm}^{-1}$ are for S-O and S=O stretching vibrations of the sulfonate groups. The bands at $2,925$ and $2,854\text{ cm}^{-1}$ are attributable to the C-H stretching vibration of dye molecule. Comparison of Fig. 3(b)-(iii) and 3(b)-(iv) points towards lesser interaction of AR73 with iron surface in the presence of urea as indicated by the lower intensity of AR73 characteristic bands. Moreover, the weak bands at 751 cm^{-1} , 898 cm^{-1} and 580 cm^{-1} in Fig. 3(b)-(iii) arising from the bending vibrations of a small amount of lepidocrocite, akagenite and magnetite, respectively, formed due to rusting of iron surface, are absent in Fig. 3(b)-(iv). This implies lesser degree of iron corrosion due to wrapping of surface by urea. AAS analysis of treated solution after 120 min of reaction reveals decrease in dissolved iron concentration from $1,024 \pm 72\text{ mg/L}$ iron at 0 mg/L urea to $655 \pm 54\text{ mg/L}$ iron at 100 mg/L urea concentration. Reduction in iron corrosion is obviously due to formation of a wrapping film of urea around ZVI surface.

4. Effect of Organic Acids

Organic acids are regularly used in many industrial dyeing processes. Fig. 4(a) and (b) shows the effect of acetic acid (CH_3COOH) and citric acid [$(\text{CH}_2)_2\text{COH}(\text{COOH})_3$], respectively, on AR73 removal, which was studied at initial solution pH 2, 3, 4 and 5. AR73 removal was enhanced in the presence of both the organic

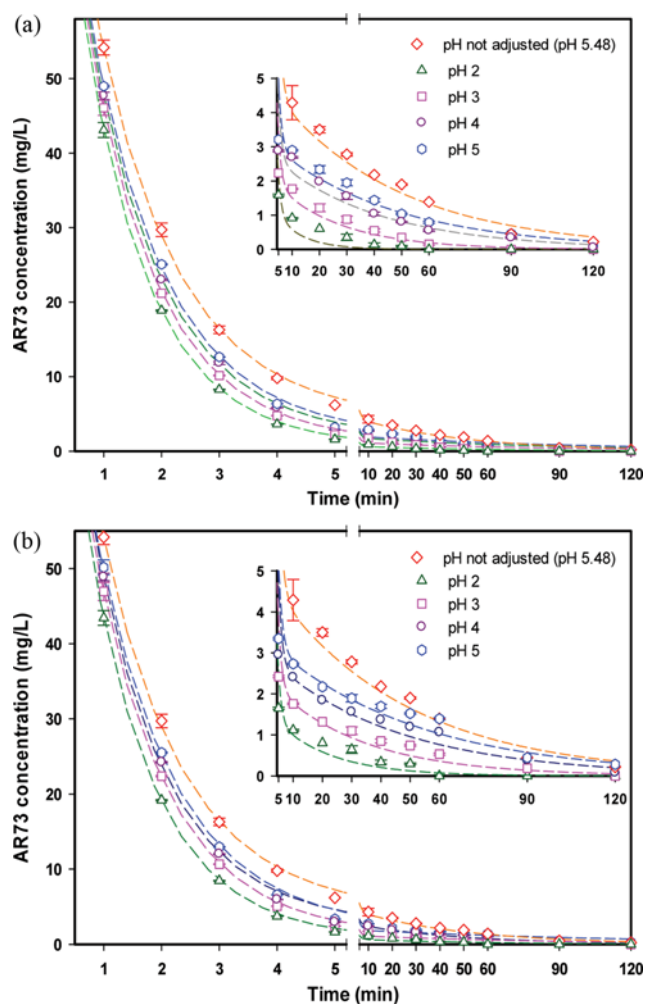


Fig. 4. Removal of AR73 by ZVI at different solution pH amended with (a) acetic acid and (b) citric acid. Inset figure shows the temporal variation in dye concentration after 5 min.

acids and highest dye removal of 98.50% and 98.35% was recorded at pH 2 within 5 min of ZVI treatment using acetic acid and citric acid, respectively. The dye removal rates, as shown in Table 2, were almost identical for both the acid systems at pH 2 but acetic acid yielded slightly better rates at higher pH systems.

Acetic acid is known to induce pitting corrosion on metals [39] and accelerated corrosion of ZVI can enhance dye conversion rate. Presence of acetic acid (HAc) enhances dissolution of ZVI by direct reduction of acetic acid on the ZVI surface according to the reaction below:



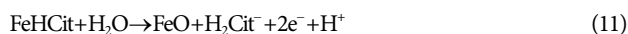
The anodic reaction occurring simultaneously at the ZVI surface, in order to balance the charge, is the dissolution of iron (Eq. (8)):



Similarly, citric acid is also reported to enhance metal corrosion and form metal-citrate complex. The dye conversion in the presence of citric acid may proceed with the following reactions:

Table 2. Biphasic AR73 removal rates in the presence of different organic acids and experimental sets

Dyebath additives	Concentration (mg/L)/pH	Removal rate (min ⁻¹)		R ²
		Initial 5 min	After 5 min	
Acetic acid	Not adjusted (pH 5.48)	0.685	0.017	0.997
	pH 2	0.876	0.067	1.000
	pH 3	0.831	0.041	0.999
	pH 4	0.805	0.025	0.999
	pH 5	0.778	0.022	0.998
Citric acid	Not adjusted (pH 5.48)	0.685	0.017	0.997
	pH 2	0.875	0.052	1.000
	pH 3	0.814	0.032	0.998
	pH 4	0.785	0.023	0.998
	pH 5	0.766	0.020	0.998
Experimental combination	A	0.685	0.017	0.997
	B	0.812	0.036	0.999
	C	0.772	0.024	0.998
	D	0.900	0.086	1.000



The generated electrons would be rapidly transferred to azo dye in addition to the electrons generated from the reduction of water molecule by ZVI, resulting into faster dye removal. AAS analysis of dye solution sampled after 120 min shows dissolved iron concentration of $1,125 \pm 42$ mg/L and $1,062 \pm 32$ mg/L iron in the pH 2 batch reactors amended with acetic acid and citric acid, respectively. The recorded values are much higher than that in the control (820 ± 44 mg/L iron) and the other pH systems suggesting greater iron corrosion. Also, acetic acid was more corrosive than citric acid.

Comparatively, lower dye removal was observed by using citric acid than acetic acid, especially at pH 3, 4 and 5. One plausible explanation comes from the relative strength of aqueous soluble complexes between $\text{Fe}^{2+}/\text{Fe}^{3+}$ and these organic ligands. Unfortunately, there is no reported stability constant value for the $\text{Fe}^{2+}/\text{Fe}^{3+}$ -acetate complex but citrate ligand forms several times tighter complexes with other metal ions, when compared to acetic acid [40]. Also, it is reported that the strength of surface adsorption and complexation increases as the number of carboxylic groups in each ligand molecule increases; hence citrate anion with more number of carboxylic groups should form tighter complex with iron oxide, which are corrosion products of ZVI [33]. The sequence of dye removal rates (Table 2) is opposite the sequence for the strength of surface adsorption and complexation of these organic ligands. Therefore, the dye removal is retarded by the stronger binding of citrate at the iron metal surfaces so that the availability of the reactive sites is decreased.

However, this complexation effect was less inhibitory at pH 2 where excessive H_2 gas bubbles, formed due to reduction of hydrogen ions on the metal surface, were observed in the presence of

both the organic acids. These H_2 gas bubbles can cause convection in the system that allows proper mixing and may facilitate removal of iron-organic acid complexes from the reactive sites on the ZVI surface, thus, improving dye removal rate [41]. Depending on the surface condition of ZVI, this H_2 gas could also function as a reductant [42,43]. Also, it has been reported that the oxide film formed in citric acid solution is thin and conductive for electron transfer [44,45]; hence, the metal oxide film (see reaction 10) in citric acid was not effective enough to disturb ZVI dissolution and its reactivity.

5. Effect of All the Additives Mixed: Model Development

Dyebath effluent is a cocktail of a large amount of salts and acids; therefore, it is important to test the efficiency of ZVI in the presence of all the chemical additives amended to the synthetic wastewater. For this, AR73 removal experiments were carried out by adding all the studied salts at their highest concentration (6 g/L

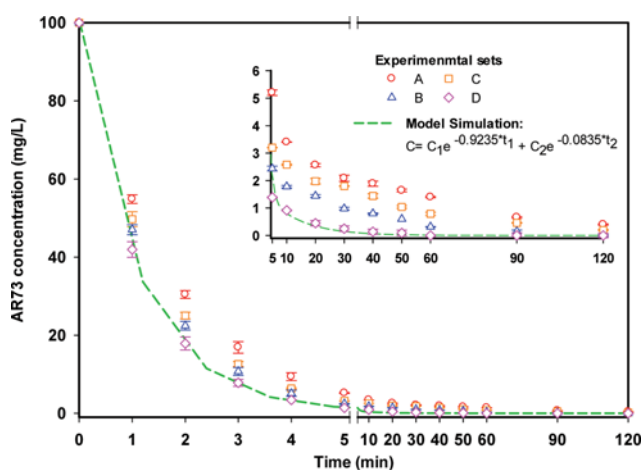


Fig. 5. Removal of AR73 by ZVI in the presence of all the additives and model simulation. Inset figure shows the temporal variation in dye concentration after 5 min.

NaCl, 2,000 mg/L $(\text{NH}_4)_2\text{SO}_4$ and 100 mg/L urea). Four different experimental sets were A (no salt or acid added, initial pH 5.48), B (with all the salts but no acid, initial pH 6.56), C (all salts, initial pH adjusted to pH 9 using 1 M NaOH) and D (all salts, initial pH of the solution adjusted to 2 using 1 : 1 mixture of acetic acid (AA) and citric acid (CA)). The results as shown in Fig. 5 and compiled in Table 2, reveal highest dye removal rate and efficiency (98.62%) in set D (in the presence of all the chemical additives), whereas lowest (94.80%) in set A (in the absence of all the additives). At alkaline pH 9, the effect of aggressive reaction boosters like Cl^- and SO_4^{2-} anion is compromised while the reaction rate was 1.3 times higher in the presence of both the acids (i.e., at pH 2) compared to the control set A, highlighting the significance of solution pH. A potential drawback of the ZVI-based technology is the rapid surface passivation (due to oxidation), which decreases its regeneration capacity. However, the presence of aggressive reaction boosters (like Cl^- and SO_4^{2-}) and acidic reaction conditions allows rejuvenation of the ZVI surface and ensures its access to the dye molecules. Furthermore, greater than 94.5% dye removal was recorded in all the experimental combinations, thus indicating the remarkable potential of ZVI in treating azo dye amended dye-bath effluents at diverse pH range. This gives ZVI an edge over ozone-based dye removal technology which is negatively impacted by the presence of dye-bath additives [46].

In the experimental combination sets A, B, C and D, the individual effect (enhancing or inhibitory) of each dye-bath additive governed the overall reaction kinetics. Hence, a conceptual model was developed considering the contribution of each dye-bath additive on the dye removal kinetics. The overall dye removal kinetics in both rapid and slow phase of dye removal represents the sum of effect of each dye-bath additive present in the wastewater, and hence, the proposed model is:

For initial rapid phase (t_1) of dye removal:

$$C_A = C_1 e^{-\{k_1 + \Delta k_1^{\text{NaCl}} - \Delta k_1^{(\text{NH}_4)_2\text{SO}_4} - \Delta k_1^{\text{Urea}} + (\Delta k_1^{\text{Acetic acid}} + \Delta k_1^{\text{Citric acid}})/2\} t_1} \quad (12)$$

For later slow phase (t_2) of dye removal:

$$C_B = C_2 e^{-\{k_2 + \Delta k_2^{\text{NaCl}} - \Delta k_2^{(\text{NH}_4)_2\text{SO}_4} - \Delta k_2^{\text{Urea}} + (\Delta k_2^{\text{Acetic acid}} + \Delta k_2^{\text{Citric acid}})/2\} t_2} \quad (13)$$

where C_A and C_B are the variation in dye concentration with time t_1 and t_2 , respectively; C_1 and C_2 are the respective dye concentration at $t=0$ min and $t=5$ min; k_1 and k_2 are AR73 removal rates without any additive for respective reaction phases; Δk_1^{NaCl} , $\Delta k_1^{(\text{NH}_4)_2\text{SO}_4}$, Δk_1^{Urea} , $\Delta k_1^{\text{Acetic acid}}$ and $\Delta k_1^{\text{Citric acid}}$ for the first phase of reaction and Δk_2^{NaCl} , $\Delta k_2^{(\text{NH}_4)_2\text{SO}_4}$, Δk_2^{Urea} , $\Delta k_2^{\text{Acetic acid}}$ and $\Delta k_2^{\text{Citric acid}}$ for the second reaction phase are the difference in the rate constants when NaCl, $(\text{NH}_4)_2\text{SO}_4$, urea, acetic acid and citric acid, respectively, were present at their highest concentration to that obtained in the absence of these additives. Since a 1 : 1 ratio of acetic acid and citric acid was used in the mixed experimental sets for adjusting the solution pH, their reaction rates were reduced to half. The model thus developed was fitted for the experimental data obtained with various dye-bath additive combinations (Fig. 5). The data of experimental set D matched well with the simulated values. Model validation statistics ($R^2=0.9995$; S.D.=31.726; R.M.S.E.=8.479; t statistic=2.044; t critical=2.160; $c^2=3.201$) also revealed that the biphasic kinetics

model fitted dye removal data from experimental set D most precisely than others and the model is unbiased.

CONCLUSIONS

The present batch investigations reveal that the occurrence of dye-bath additives in effluent could affect the reactivity of ZVI towards azo dyes. Na^+ induces 'salting out' effect on the dye molecules in the bulk solution, while Cl^- enhances the electron transfer process in the bulk solution and induces pitting corrosion of ZVI surface. All these effects led to improved AR73 removal rate in the presence of NaCl. $(\text{NH}_4)_2\text{SO}_4$ benefitted the reaction rates till 1,000 mg/L concentration, beyond which it retarded the reaction rate. At low concentration, 'salting out' effect of $(\text{NH}_4)_2\text{SO}_4$ on the bulk solution, enhanced iron corrosion by aggressive SO_4^{2-} anion, and reducing effect of 'sulfate green rust' complemented to enhanced dye removal rates. However, beyond 1,000 mg/L $(\text{NH}_4)_2\text{SO}_4$ concentration, both NH_4^+ and SO_4^{2-} could compete with azo dye molecules in occupying the adsorptive and reactive sites on the iron surface. Resulting complex formation, in higher scale, inhibited the mass transfer of dye molecules and compromised the reaction rates. Urea drastically reduced the dye removal rate by virtue of its chaotropic effect on the bulk dye solution and also because it forms a wrapping film around ZVI surface, as revealed by FTIR analysis. Increased iron corrosion in the presence of acetic acid and citric acid enhanced the reactivity of ZVI. The reduction rate followed the decreasing order acetic acid > citric acid, to the stronger complex forming ability of citrate anion. Dye removal was greatly enhanced at acidic pH 2 in the presence of all the additives while at alkaline pH 9 the dye removal rate was compromised, pointing towards the dominant role of solution pH.

The dye removal kinetics was biphasic with initial rapid phase followed by slow phase. The experimental data could be well evaluated using biphasic rate equation showing high values of regression coefficients ($R^2 > 0.995$ in all the cases) in all the cases. AR73 removal in the presence of all the selected additives could be modelled by taking into account the individual effect of all the additives and the biphasic model simulation fitted well with the data of experimental set D. These results may serve to indicate different strategies to treat acid dye-bath effluent in real processes where pH is acidic in general and the presence of additives may significantly affect the benefits achieved by ZVI-mediated water treatment.

REFERENCES

1. J. Fan, Y. Guo, J. Wang and M. Fan, *J. Hazard. Mater.*, **166**, 904 (2009).
2. M. Ghaedi, E. Alam barakat, A. Asfaram, B. Mirtamizdoust, A. A. Bazrafshan and S. Haiati, *RSC Adv.*, **5**, 42376 (2015).
3. F. Nasiri Azad, M. Ghaedi, K. Dashtian, S. Haiati, A. Goudarzi and M. Jamshidi, *New J. Chem.*, **39**, 7998 (2015).
4. M. Jamshidi, M. Ghaedi, K. Dashtian, A. M. Ghaedi, S. Hajati, A. Goudarzi and E. Alipanahpour, *Spectrochim. Acta Mol. Biomol. Spectrosc.*, **153**, 257 (2016).
5. E. Alipanahpour Dil, M. Ghaedi, A. M. Ghaedi, A. Asfaram, A. Goudarzi, S. Hajati, M. Soylak, S. Agarwal and V. K. Gupta, *J. Ind.*

- Eng. Chem.*, **34**, 186 (2016).
6. A. Asfaram, M. Ghaedi, S. Hajati and A. Goudarzi, *RSC Adv.*, **5**, 72300 (2015).
 7. A. Asfaram, M. Ghaedi, S. Hajati, A. Goudarzi and A. A. Bazrafshan, *Spectrochim. Acta Mol. Biomol. Spectrosc.*, **145**, 203 (2015).
 8. S. Mosleh, M.-R. Pahimi, M. Ghaedi, K. Dashtian and S. Hajati, *RSC Adv.*, **6**, 17204 (2016).
 9. A. Al-Kdasi, A. Idris, K. Saed and C. T. Guan, *Global Nest: the Int. J.*, **6**, 222 (2004).
 10. H. S. Rai, M. S. Bhattacharyya, J. Singh, T. K. Bansal, P. Vats and U. C. Banerjee, *Crit. Rev. Environ. Sci. Tec.*, **35**, 219 (2015).
 11. C. Audí-Miró, S. Cretnik, C. Torrentó, M. Rosell, O. Shouakar-Stash, N. J. Otero, E. M. Palau and A. Soler, *J. Hazard. Mater.*, **299**, 747 (2015).
 12. A. Sinha and P. Bose, *J. Colloid Interface Sci.*, **314**, 552 (2007).
 13. A. Sinha and P. Bose, *Environ. Eng. Sci.*, **28**, 701 (2011).
 14. A. R. Esfahani, S. Hojati, A. Azimi, L. Alidokht, A. Khataee and M. Farzadian, *Korean J. Chem. Eng.*, **31**, 630 (2014).
 15. R. Kumar and A. Sinha, *IJRET*, **2**, 227 (2013).
 16. M. R. Sohrabi, S. Amiri, H. R. F. Masoumi and M. Moghri, *J. Ind. Eng. Chem.*, **20**, 2535 (2014).
 17. Y. Choi, B. Park and D. K. Cha, *Korean J. Chem. Eng.*, **32**, 1812 (2015).
 18. R. Kumar and A. Sinha, *Desalin. Water Treat.*, **57**, 3205 (2016).
 19. R. Kumar and A. Sinha, *J. Environ. Sci.*, DOI:10.1016/j.jes.2016.04.002.
 20. W. Ingamells, *Color for Textiles-A User's Handbook*, Society of Dyers and Colorists, Bradford (1993).
 21. N. Efecan, T. Shahwan, A. E. Eroglu and I. Lieberwirth, *Desalination*, **249**, 1048 (2009).
 22. J. D. Hamlin, D. A. S. Phillips and A. Whiting, *Dyes Pigment.*, **41**, 137 (1999).
 23. Y. Su, C. Y. Hsu and Y. Shih, *Chemosphere*, **88**, 1346 (2012).
 24. J. S. Kim, P. J. Shea, J. E. Yang and J. E. Kim, *Environ. Pollut.*, **147**, 634 (2007).
 25. Y. Wang, G. Cheng, W. Wu, Q. Qiao, Y. Li and X. Li, *Appl. Surf. Sci.*, **349**, 746 (2015).
 26. S. L. Clegg and P. Brimblecombe, *Geochim. Cosmochim. Acta*, **54**, 3315 (1990).
 27. J. H. Fan, H. W. Wang, D. L. Wu and L. M. Ma, *J. Chem. Technol. Biotechnol.*, **85**, 1117 (2010).
 28. S. Choe, H. M. Liljestrand and J. Khim, *Appl. Geochem.*, **19**, 335 (2004).
 29. J. Zou, *Arsenic removal from groundwater with iron tailored granular activated carbon preceded by pre-corroded steel* (Ph.D. Thesis), Pennsylvania State U., University Park, PA (2009).
 30. J. Choi, B. Batchelor, C. Won and J. Chung, *Chemosphere*, **86**, 860 (2012).
 31. P. Ph. Remy, M. Etique, A. A. Hazotte, A. S. Sergent, N. Estrade, C. Cloquet, K. Hanna and F. P. A. Jorand, *Water Res.*, **70**, 266 (2015).
 32. S. J. Hug, *J. Coll. Inter. Sci.*, **188**, 415 (1997).
 33. C. Su and R. W. Puls, *Environ. Sci. Technol.*, **38**, 2715 (2004).
 34. J. Shore, *Colorants & Auxiliaries* (Vol. 2), Society of Dyers and Colorists, Bradford, 442 (1990).
 35. K. Das, N. Sarkar, S. Das, A. Datta, D. Nath and K. Bhattacharyya, *J. Chem. Soc., Faraday Trans.*, **92**, 4993 (1996).
 36. J. Zhang, G. Zhang, K. Zheng, D. Cai and Z. Wu, *J. Nanosci. Nanotechnol.*, **15**, 6103 (2015).
 37. A. Idrissi, P. Damay, K. Yukichi and P. Jedlovsky, *J. Chem Phys.*, **129**, 164512 (2008).
 38. M. Styliidi, D. I. Kondarides and X. E. Verykios, *Appl. Catal. B*, **40**, 271 (2003).
 39. H. H. Hassan and K. Fahmy, *Int. J. Electrochem. Sci.*, **3**, 29 (2008).
 40. A. E. Martel, R. M. Smith and R. J. Motekaitis, *NIST standard reference database 46 version 7.0: NIST critically selected stability constants of metal complexes*, In: NIST Standard Reference Data, Gaithersburg, MD (2003).
 41. S. Nishide and M. Shoda, *Energy Environ. Res.*, **2**, 31 (2012).
 42. D. P. Siantar, C. G. Schreier, C. S. Chou and M. Reinhard, *Water Res.*, **30**, 2315 (1996).
 43. P. Bruzzoni, R. M. Carranza and J. R. Collet Lacoste, *Int. J. Hydrogen Energy*, **25**, 61 (2000).
 44. B. F. Giannetti, P. T. A. Sumodjo and T. Rabockai, *J. Appl. Electrochem.*, **20**, 672 (1990).
 45. S. S. Abdel Rehim, S. M. Sayyah and M. M. El Deeb, *Mater. Chem. Phys.*, **80**, 696 (2003).
 46. M. Muthukumar and N. Selvakumar, *Dyes Pigment.*, **62**, 221 (2004).